The Astrophysical Journal, 777:159 (7pp), 2013 November 10 doi:10.1088/0004-637X/777/2/159

QUASI-PERIODIC WIGGLES OF MICROWAVE ZEBRA STRUCTURES IN A SOLAR FLARE

Sijie Yu[1], V. M. Nakariakov[2,3,4], L. A. Selzer[2], Baolin Tan[1], and Yihua Yan[1]
[1] Key Laboratory of Solar Activity, National Astronomical Observatories Chinese Academy of Sciences, Beijing 100012, China; sjyu@nao.cas.cn
[2] Centre for Fusion, Space and Astrophysics, Physics Department, University of Warwick, Coventry CV4 7AL, UK
[3] School of Space Research, Kyung Hee University, Yongin, 446-701 Gyeonggi, Korea
[4] Central Astronomical Observatory at Pulkovo of RAS, 196140 St Petersburg, Russia
Received 2013 August 7; accepted 2013 September 18; published 2013 October 24

ABSTRACT

Quasi-periodic wiggles of microwave zebra pattern (ZP) structures with periods ranging from about 0.5 s to 1.5 s are found in an X-class solar flare on 2006 December 13 at the 2.6–3.8 GHz with the Chinese Solar Broadband Radio Spectrometer (SBRS/Huairou). Periodogram and correlation analysis show that the wiggles have two to three significant periodicities and are almost in phase between stripes at different frequencies. The Alfvén speed estimated from the ZP structures is about 700 km s^{-1}. We find the spatial size of the wave-guiding plasma structure to be about 1 Mm with a detected period of about 1 s. This suggests that the ZP wiggles can be associated with the fast magnetoacoustic oscillations in the flaring active region. The lack of a significant phase shift between wiggles of different stripes suggests that the ZP wiggles are caused by a standing sausage oscillation.

Key words: Sun: flares – Sun: oscillations – Sun: radio radiation

Online-only material: color figures

1. INTRODUCTION

Quasi-periodic pulsations (QPPs) are a frequently observed phenomenon in the electromagnetic emission generated by solar and stellar flares in a vast energy range from radio to hard X-ray and gamma-ray bands (see Nakariakov & Melnikov 2009; Nakariakov et al. 2010; Tan et al. 2010 for recent reviews). Typically, QPPs appear as a pronounced oscillatory pattern in the intensity of the radiation with typical periods ranging from a fraction of a second to several minutes. Also, QPPs have been found as oscillations of the Doppler shift of the emission lines associated with the hot plasma in flaring sites (Mariska 2006) or the density of the plasma (Kim et al. 2012). The variety of the characteristic periods and modulation depths of QPPs suggests that they can be caused by several different mechanisms, including wave–particle interaction (e.g., Aschwanden 1987), spontaneous or driven periodic regimes of magnetic reconnection (e.g., Tajima et al. 1987; Nakariakov et al. 2010), magnetohydrodynamic (MHD) oscillations (e.g., Nakariakov & Melnikov 2009), or oscillations in an equivalent *LCR* circuit (e.g., Zaitsev & Stepanov 2008). Revealing the mechanisms responsible for the production of QPPs remains an important task in the context of our understanding of the basic physical processes operating in solar and stellar flares.

Another interesting phenomenon of flaring microwave emission is the zebra pattern (ZP) structures of the broadband spectral observations: sets of almost-parallel stripes superposed on microwave type II and IV bursts with slow frequency drifting and variations (e.g., Chernov 2006). A similar phenomenon is an "evolving emission line" (EEL), which, in contrast with the ZP, consists of a single emission stripe in the dynamical spectrum (Chernov et al. 1998; Ning et al. 2000a). There is no broadly accepted interpretation for the ZP, although recent observational findings favor the model associating ZP with the coherent generation of upper-hybrid waves at multiple double plasma resonances (DPRs) in a non-uniform plasma (Zheleznyakov & Zlotnik 1975). In this model, the frequency separation of adjacent stripes in a ZP is directly proportional to the electron gyrofrequency and hence to the magnetic field strength. This property provides us with a unique method for measuring the coronal magnetic field. The model based upon the double plasma resonance is supported by some observational evidence (e.g., Zlotnik et al. 2003; Chen & Yan 2007; Chen et al. 2011; Yu et al. 2012). However, other proposed mechanisms, e.g., based upon the whistler wave packets (e.g., Chernov 2006) and trapped upper-hybrid *Z*-mode waves (LaBelle et al. 2003) have not been ruled out. In addition, very recently Karlický (2013) proposed a new model that links ZP with propagating compressive MHD waves.

Analysis of some ZPs indicates the presence of periodic modulation. In particular, Chernov et al. (2005) found that the intensity of ZP stripes observed on 2002 April 21 pulsated quasi-periodically—the bright ZP stripes consisted of separate short-duration pulses with a period of about 30 ms. Pulsations of the same intensity in adjacent stripes were found to be similar. The detected periodicity was associated with the oscillatory nonlinear interaction of whistlers with ion–sound and Langmuir waves. That ZP event obtained great attention and the QPPs of this intensity have been considered in several follow-up studies that addressed temporal characteristics of the pulses and their polarizations (e.g., Chen & Yan 2007; Kuznetsov 2008). Chen & Yan (2007) proposed that the pulsations were associated with relaxation oscillations in a system of an electron beam and plasma waves. Kuznetsov & Tsap (2007) linked the pulsations with the periodic injection of electron beams. Kuznetsov (2008) interpreted the quasi-periodic patterns in terms of downward-propagating fast magnetoacoustic waves. A similar model was recently employed to interpret the phenomenon of fiber bursts in the dynamical spectra of flare-generated radio emissions (Karlický et al. 2013). Variations of the intensity with longer periods, about 275 ms, were detected in the event on 1998 April 15 by Ning et al. (2000a).

Another less-studied type of ZP modulation is the periodic quasi-coherent oscillating drift of the spectral stripes, also called "wiggling." In the unusually long radio event on 1992 February 17 observed with ARTEMIS, OSRA, and IZMIRAN in the 100–500 MHz band, Chernov et al. (1998) detected pronounced wiggling of the ZP with a period of about three minutes, with a frequency variation amplitude of about 5 MHz. The relative amplitude of the spectral variation was 2%. It was linked with

the possible variation of the emitting plasma density by about 4% or of the magnetic field by 2%, or a combination of both. An EEL observed simultaneously with the ZP showed a similar variability. In the event of 1998 April 15 observed with Huairou at about 3 GHz, Ning et al. (2000a, 2000b) and Chernov et al. (2001) found that the central frequencies of the stripes fluctuated on a typical timescale of 0.5 s and 1.5–2 s in two different time intervals. In the shorter period case, three stripes were found to wiggle synchronously by about 200 MHz with a relative frequency variation of about 6%. It was estimated to correspond to the relative variation of the magnetic field of 10% or the density of about 6%. In the longer period case, the spectral amplitude of the oscillations was 80 MHz, from 3.41 GHz to 3.49 MHz. A similar wiggling evolution of ZP stripes can be seen in Figure 8 of Chen et al. (2011) and has not yet been analyzed in detail. Visual inspection of the figures shows that the period is about 0.3 s and the amplitude is about 20 MHz, which is about 1.5% of the central frequency of 1.35 GHz.

Generally, the periods detected in ZP fine structure wiggling coincide, by an order of magnitude, with the transverse fast magnetoacoustic crossing time in a typical loop of a coronal active region (e.g., De Moortel & Nakariakov 2012). Moreover, the required amplitudes of the variations of the magnetic field and/or the plasma density of a few percent, are consistent with those observed in these waves in other bands (e.g., Williams et al. 2001). Thus, it is natural to expect that the periodicity may be associated with either an impulsively generated fast magnetoacoustic wave train (e.g., Roberts et al. 1984; Nakariakov et al. 2004) or with a standing sausage mode of a fast magnetoacoustic resonator (e.g., Kopylova et al. 2007; Zaitsev & Stepanov 2008; Nakariakov et al. 2012), or result from the passage of a perpendicular fast wave through a randomly structured coronal plasma (Nakariakov et al. 2005). All these mechanisms are of great interest for MHD coronal seismology, as they bring us the unique information about fine, unresolved structuring of the coronal plasma and can rarely be studied in the EUV band because of its insufficient time resolution.

The aim of this paper is to perform a detailed study of the quasi-periodic wiggles in a microwave ZP observed in a solar flare. In Section 2, the instrumentation and the data analyzed are described. In Section 3, we present the findings that are then discussed in Section 4.

2. OBSERVATIONAL DATA

The flare analyzed in this paper occurred on 2006 December 13 in NOAA active region 10930 located on disk (S05W33). It was a typical two-ribbon flare that reached the *GOES* level X3.4/4B class at about 02:40 UT (Isobe et al. 2007; Yan et al. 2007). This flare was observed by *Solar and Heliospheric Observatory* (*SOHO*), *Transition Region and Coronal Explorer* (*TRACE*), *Hinode*, and *RHESSI* satellites. It was also well observed by the ground-based Chinese Solar Broadband Radio Spectrometer (SBRS/Huairou; Tan et al. 2007; Yan et al. 2007) and the Nobeyama Radioheliograph (NoRH). SBRS/Huairou (Fu et al. 1995, 2004; Yan et al. 2002) is a robust solar radio spectrometer that measures the total flux density of solar microwave emission on both left- and right-handed circular polarization (LHCP and RHCP) at three frequency bands: 1.10–2.06 GHz (time resolution of 5 ms and frequency resolution of 4 MHz), 2.6–3.8 GHz (8 ms and 10 MHz), and 5.20–7.60 GHz (5 ms and 20 MHz). NoRH can provide imaging observations at frequencies of 17 GHz and 34 GHz (Nakajima et al. 1994). Thirteen ZP structures were recorded by SBRS/Huairou at 2.6–3.8 GHz during the flaring process in the discussed event (Yu et al. 2012). Here we focus on the time interval 02:40–03:05 UT after the soft X-ray emission maximum. Two long-lasting ZPs were detected at 02:43:00–02:43:20 UT (ZP1) and 03:03:00–03:03:20 UT (ZP2) that show quasi-periodic spectral wiggling of the ZP stripes (see Figures 1(a)–(b)).

The left panel in Figure 2 shows the full disk EUV image at 195 Å obtained by the Extreme-ultraviolet Imaging Telescope (EIT; Delaboudinière et al. 1995) onboard *SOHO* during the decay phase of the flare with an inset of the *TRACE* (Handy et al. 1999) image at 195 Å showing the post-flare loop arcade with explosive features at the time of ZP2. The right panel shows the NoRH 17 GHz full disk intensity image and an inset of the enlarged 17 GHz image superposed with a 34 GHz image. The source region of the radio emission at 17 GHz has approximately the same position as the EUV arcade structure in the flare region during the decay phase with the maximum situated in the northeast of the arcade, between the opposite footpoints of 34 GHz radio sources. The spatial separation of the footpoints is about 50 arcsec. The NoRH 17 GHz full disk image shows that AR 10930 is a unique strong radio emission source on the solar disk in this flare event, indicating that the radiation of the ZPs possibly comes from the flare core region.

The extended duration ($t > 15$ s) of ZP1 and ZP2 makes it possible to study their long-term variation, including the wiggling of individual spectral stripes. To analyze the oscillatory patterns in ZPs, we need to extract the ZP stripes from the background emissions in the raw microwave spectrogram. Specific steps of the data processing are illustrated in Figure 1. The microwave dynamic spectrograms of ZP1 and ZP2 in the LHCP are shown in Figures 1(a)–(b). Note that the RHCP spectrograms are not used for large saturation in the low-frequency range (<2.9 GHz). The first step of processing is to remove the trend of the background emission to make the bright stripe-like features prominent. For that, a running average smoothed over 10 pixels is subtracted from the frequency profile at each instant of time. We subsequently apply a low-pass filter to smooth out the separate spike-like structures in the stripes. We then use the thresholding method to segment the stripe features as shown in Figures 1(c)–(d). The following step is the data series extraction. We fit a Gaussian to the frequency profile of each stripe and then normalize the Gaussians to their amplitudes so that the brightness of stripes is uniform. This procedure removes the information about the amplitude modulation of the signal while highlighting the frequency modulation. The centers of the Gaussian peaks give us the instant radio-frequencies of the stripes. After that, we track the frequency data series of several of the longest stripes that have been identified manually. The variation of the centers of the best-fitted Gaussians in time allows us to obtain the "skeletons" $f_N(t)$ of the frequency modulation of the individual spectral stripes in the analyzed ZPs ($N = 1, 2, 3\ldots$). Note that here N denotes the Nth extracted stripe enumerated from the highest observed frequency to the lowest frequency in the spectrogram. Also, one can study the time variation of the difference $\Delta f_N = f_{N+1} - f_N$ between neighboring stripes. Figures 1(e)–(f) shows the rescaled Gaussian image superimposed with the spectral skeletons of the four stripes of the highest frequencies. Note that as the third extracted stripe in ZP2 was seen to be gapped at 03:03:05–03:03:06 UT in the raw spectrogram (Figure 1(b)) and the high contrast image (Figure 1(d)), and we needed to connect the two segments with a straight line.

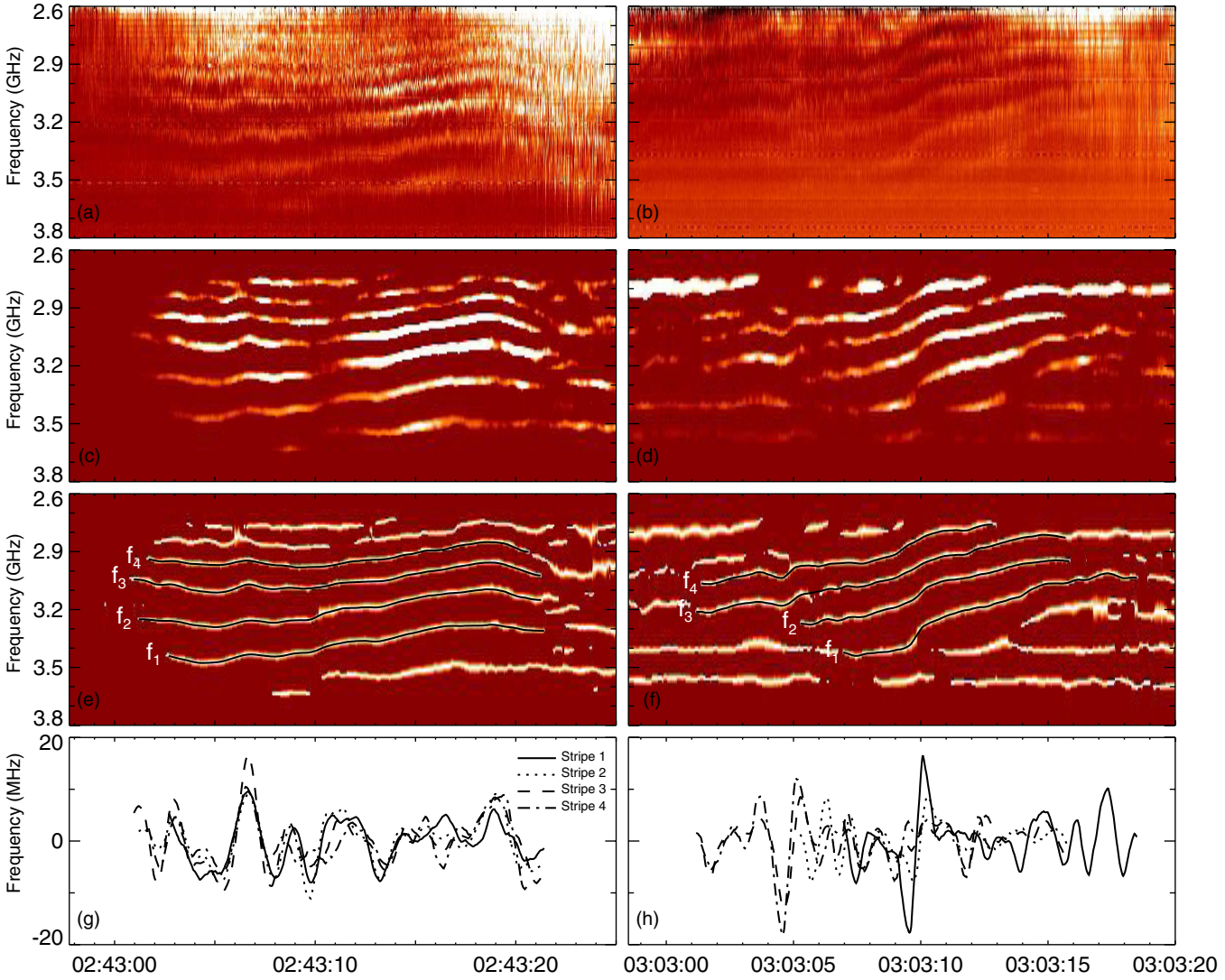

Figure 1. Zebra pattern structures on 2006 December 13 observed by SBRS/Huairou at 2.6–3.8 GHz and the illustration of the processes of extracting the zebra pattern stripes. Panels (a) and (b): raw spectrograms at 2.6–3.8 GHz on LHCP; (c) and (d) high contrast images; (e) and (f) rescaled images with the extracted stripes superposed; and (g) and (h) detrended stripes frequency f_N.

(A color version of this figure is available in the online journal.)

3. RESULTS

The presence of wiggling oscillatory patterns in the two microwave ZPs is seen in the time variation of the spectral skeletons. To quantify this finding, we performed periodogram and autocorrelation analyses of the f_N and Δf_N time profiles of the extracted stripes. The f_N time profiles were first smoothed by 30 points (0.24 s) to remove high-frequency noise and then detrended by subtracting the signal f_N smoothed with a 100 point (0.8 s) boxcar. The detrended time profiles are shown in Figures 1(g)–(h). Note that the smoothing of f_N attenuates the signal amplitude of oscillation. The oscillation amplitude of f_N without smoothing is about 20 MHz, larger than the frequency resolution of the spectrum (10 MHz). Power spectra of the pre-processed signals were obtained with the use of the Lomb–Scargle periodogram (e.g., Scargle 1982; see the left panels of Figures 3–4). The spectra contain significant peaks above the 99.99% confidence level. Additional confirmation of the significance of the detected oscillations was obtained by the application of Fisher's randomization test (Linnell Nemec & Nemec 1985; Yuan et al. 2011). The calculation of the spectral peaks for 200 permutations confirmed that the significance of the main peaks was greater than 99%. To avoid the appearance of artificial periodicities due to the smoothing procedure, we calculated the periodograms of the f_N time profiles obtained for a set of noise-removing boxcars (10, 20, 30 points) and trend-removing boxcars (60, 70, 80, 100 points; see Kupriyanova et al. 2010 for a discussion of this method). The positions of pronounced spectral peaks in the periodograms do not show any dependence on the smoothing width, implying that these spectral peaks are not artifacts of the smoothing.

Figure 3(a) presents the periodograms of the f_N time profiles of four highest-frequency stripes in ZP1 with the long-term trend removed. There are two well-pronounced spectral peaks in the vicinities of 0.70 and 1.20 Hz ($P_1 \sim 1.43$ s and $P_2 \sim 0.83$ s) that are seen in all four stripes. The four auto-correlation functions versus time lag (Figure 3(b)) show evident in-phase periodic behavior over several periods. In the auto-correlation functions, the period P_1 is well seen in all stripes, while the period P_2 is pronounced only in f_3 and f_4. Figure 3(c) presents the periodograms of time profiles of detrended spectral difference of the stripes Δf_N. The three profiles of Δf_N show different periodic

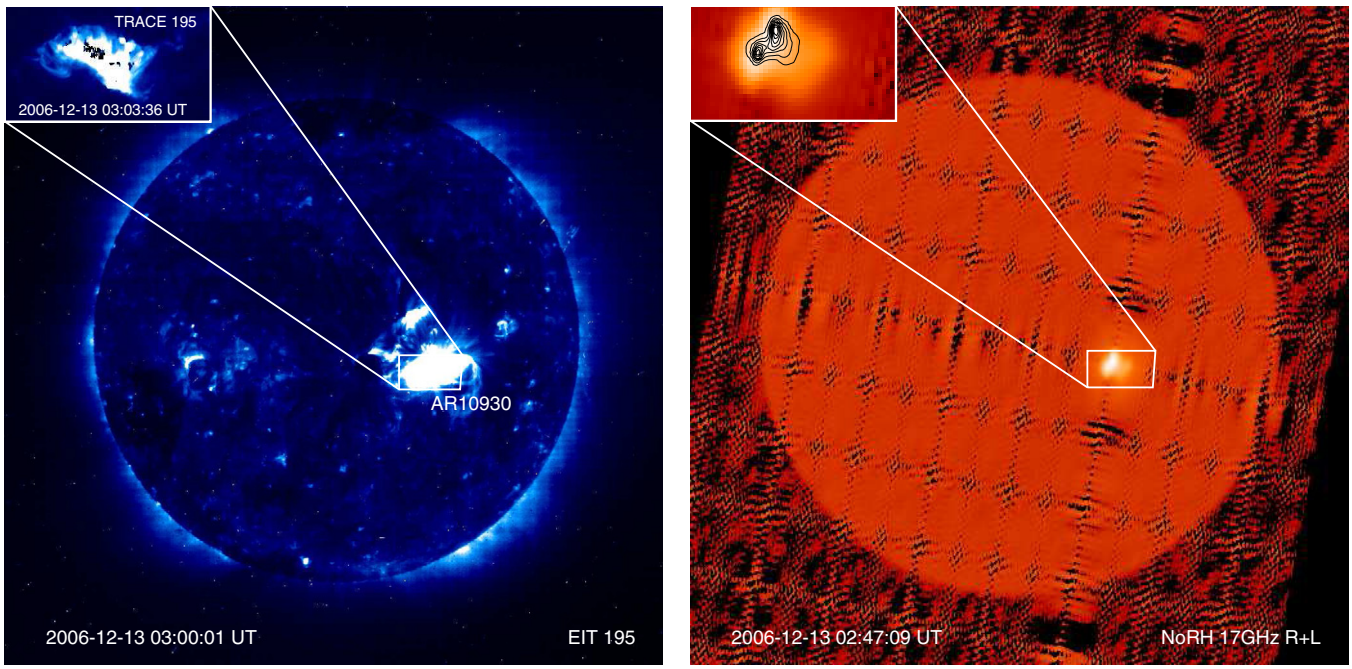

Figure 2. Full disk *SOHO*/EIT 195 Å at 03:00:01 UT and NoRH 17 GHz intensity images at 02:47:09 UT on 2006 December 13. Insets show the *TRACE* 195 Å image and the enlarged NoRH 17 GHz image of AR 10930.

(A color version of this figure is available in the online journal.)

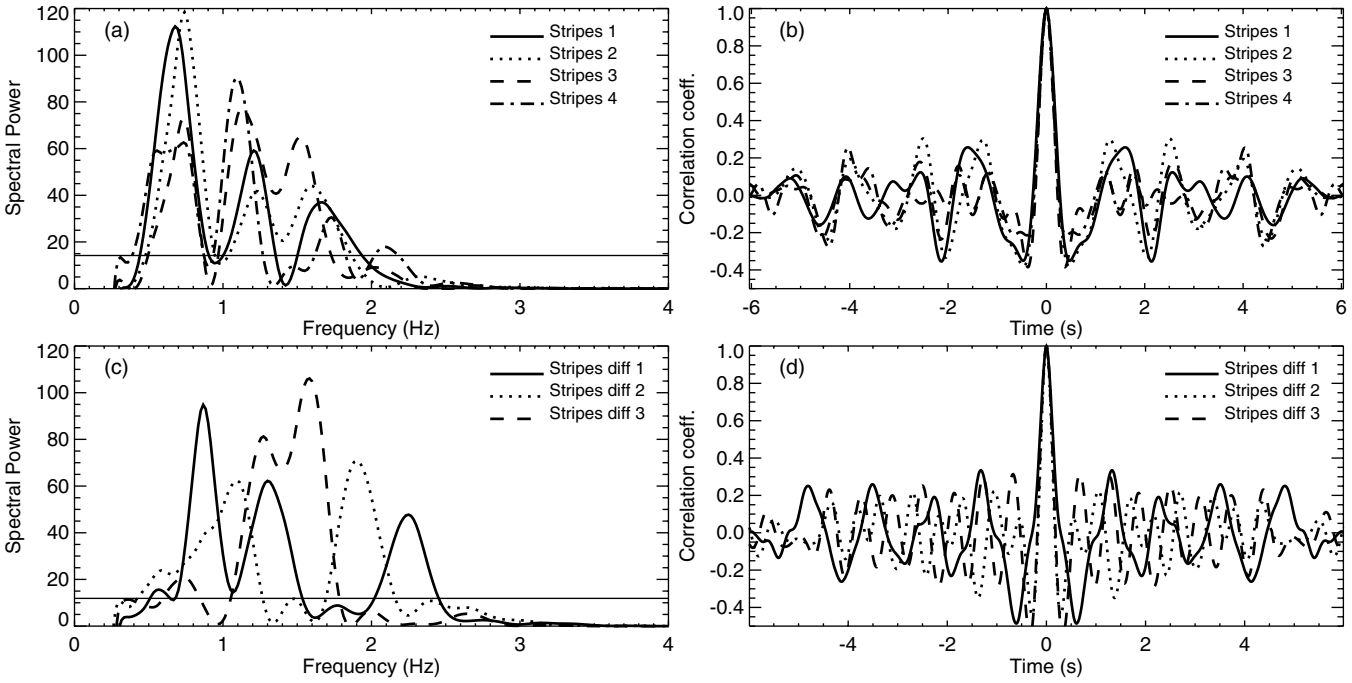

Figure 3. Periodograms and auto-correlation functions of QPP components of (a) and (b) the stripe frequency f_N, and (c) and (d) the frequency separation Δf_N of two neighboring stripes in the ZP1. Horizontal lines in the periodograms indicate a 99.99% confidence level.

behaviors with three dominant peaks in the vicinities of 0.86, 1.58, and 1.90 Hz (1.16, 0.63 and 0.53 s). In Figure 3(d), the auto-correlation functions of detrended Δf_s show still significant though less pronounced periodic oscillatory patterns than were obtained for the central frequencies of the stripes. The spectral differences $\Delta f_{3,4}$ between the second and third stripes and the third and the fourth stripes (dashed and dotted curves, respectively) have periods that are apparently two times shorter than the difference between the first and second stripes Δf_2.

Figure 4(a) shows the periodograms of the detrended f_N time profiles of the four highest-frequency stripes in ZP2. Two pronounced common peaks are seen in the vicinities of 1.20 and 1.70 Hz ($P_2 \sim 0.83$ s and $P_3 \sim 0.59$ s). The periodicity of P_2 is not detected in the detrended time profile of f_2. The auto-correlation functions of the detrended f_N time profiles all have pronounced oscillatory patterns over several periods (Figure 4(b)). Periods P_2 and P_3 are present in the auto-correlation function of f_1, f_3, and f_4. Figure 4(c) presents the

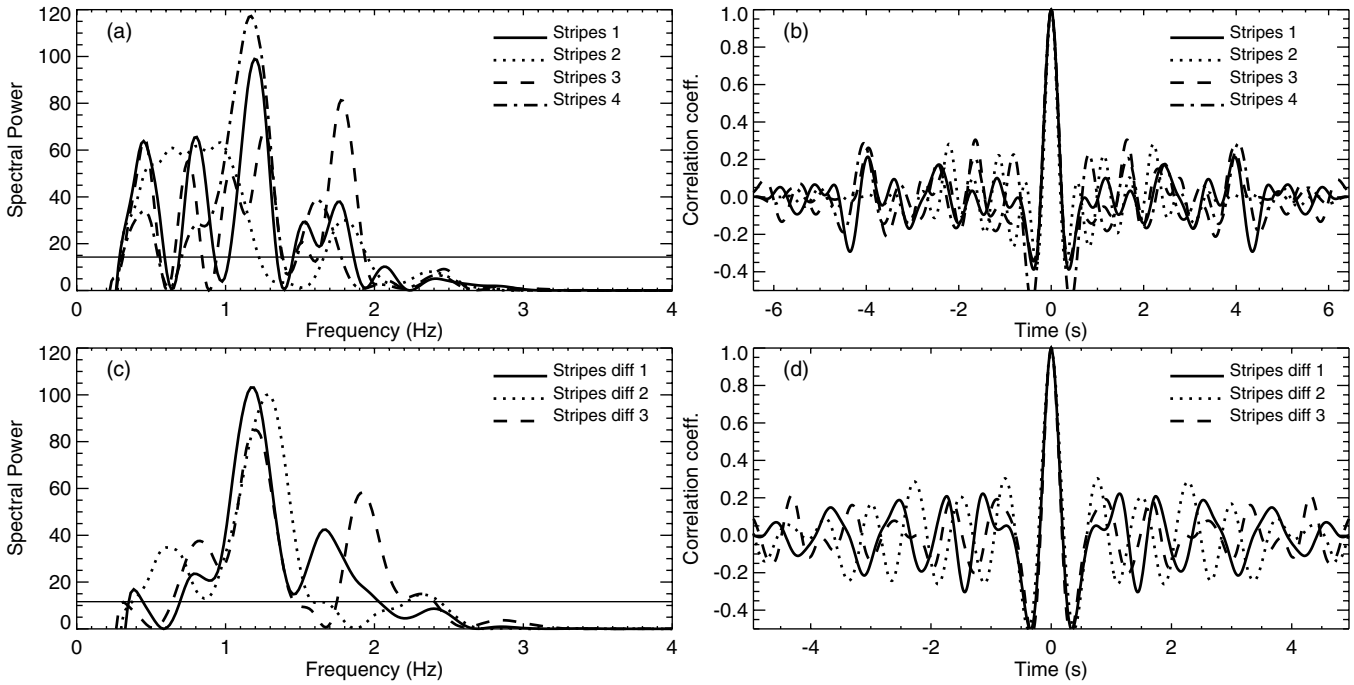

Figure 4. Same as in Figure 3 for ZP2.

periodograms of time profiles of detrended Δf_N, showing an obvious peak at 1.20 Hz ($P_2 \sim 0.83$ s). The auto-correlation functions in Figure 4(d) have a similar periodicity for all the three Δf_N.

Additionally, as we can see in Figures 3 and 4, the periodograms and auto-correlation functions of the detrended f_N and Δf_N time profiles in ZP1 and ZP2 all have a well-pronounced common spectral peak at the period $P_2 \sim 0.83$ s. The observed amplitude of the frequency variation in the ZP wiggles is about 20 MHz, about 0.7% of the central frequency.

To establish phase relations between the periodic wiggles of neighboring stripes, we calculate the cross-correlation coefficients of the detrended time profiles of f_N. For ZP1, the highest cross-correlation coefficients—0.86 between stripes 1 and 2, 0.85 between stripes 2 and 3, and 0.85 between stripes 3 and 4—are obtained for the time lags less than 0.01 s. Likewise, for ZP2, the highest cross-correlation coefficients are 0.79 between stripes 1 and 2, 0.56 between stripes 2 and 3, and 0.84 between stripes 3 and 4 for the time lags 0.12 s, −0.02 s, and −0.02 s, respectively. Thus, we can accept that the ZP wiggles occur almost in phase, as in all cases the time lag is found to be much smaller than the oscillation period and is likely to be attributed to noise.

4. DISCUSSIONS AND CONCLUSION

Analysis of the fine spectral structure of individual stripes in two microwave ZPs observed with SBRS/Huairou shows that central frequencies of the stripes perform quasi-periodic oscillations (wiggling) in the range from about 0.5 s to 1.5 s. Simultaneously, the oscillations are found to have two to three significant periodicities. Similar periodicities are detected in the spectral differences of neighboring ZP stripes. The frequency variation amplitude is about 20 MHz, giving a relative amplitude of 0.7%. Both the wiggling periods and amplitudes are consistent with previous reports of this effect in Chernov et al. (1998, 2001) and Ning et al. (2000a, 2000b). Wiggling of neighboring stripes is found to be almost in phase.

The detected periods are of the order of the transverse Alfvén or fast magnetoacoustic transit time in active region loops and other plasma non-uniformities (for a typical spatial scale of 1 Mm and Alfvén speed of 1 Mm s^{-1}). This timescale plays an important role in the physics of MHD wave interaction with structured plasma. In particular, an impulsively excited fast magnetoacoustic disturbance of a coronal loop or a current sheet develops in a quasi-periodic wave train with a period about the same as the transverse fast magnetoacoustic transit time (Roberts et al. 1984; Nakariakov et al. 2004; Jelínek et al. 2012). Also, this timescale is a typical period of standing sausage fast magnetoacoustic modes of such a loop in a leaky regime (Kopylova et al. 2007; Nakariakov et al. 2012). Thus, it is reasonable to assume that the observed periodicities could be connected with MHD wave dynamics.

Consider the DPR model (see, e.g., Zheleznyakov & Zlotnik 1975; Kuznetsov & Tsap 2007) as the mechanism responsible for the generation of ZPs. According to the DPR model, the microwave ZP structure is likely to be interpreted as a great enhancement of electrostatic upper-hybrid waves at certain resonance levels where the upper-hybrid frequency f_{uh} is equal to the harmonics of electron cyclotron frequency f_{ce}:

$$f_{uh} = \left(f_{pe}^2 + f_{ce}^2\right)^{1/2} \simeq s f_{ce}, \quad (1)$$

where f_{pe} is the plasma frequency of electrons and s is an integer harmonic number. We would like to stress that the index s used here is different from the index N used above. Enumeration of the observed ZP stripes with index N begins from the stripe of the highest observed frequency, while some higher-frequency stripes can be missing. Hence, $N = s - M$, where M is the number of missing stripes.

If the plasma density and the absolute value of the magnetic field, and hence the electron plasma and cyclotron frequencies, vary with height, there are several spatially separated levels

where the DPR condition is satisfied. Radio emissions from different DPR levels come at the local upper-hybrid frequencies. The emissions from different DPR levels form different individual stripes of the ZP structure. When taking into account that $f_{pe} \gg f_{ce}$, i.e., the upper-hybrid frequency $f_{uh} \simeq f_{pe}$, the emission frequency f_s of a ZP stripe at harmonics s equals the plasma frequency f_{pe} or its harmonic. The frequency separation between neighboring ZP stripes at harmonics s and s + 1 is

$$\Delta f_s = f_{s+1} - f_s \simeq \frac{m}{1 - (2L_n/L_B)} f_{ce}, \quad (2)$$

where $L_n = n_e(\partial n_e/\partial h)^{-1}$ and $L_B = B(\partial B/\partial h)^{-1}$ at the height h; B and n_e are the magnetic field and the plasma density, respectively, that are non-uniform in the vertical direction. Hence we obtain

$$f_s \simeq m f_{pe} \sim n_e^{1/2}, \quad (3)$$

$$\Delta f_s \sim m f_{ce} \sim B. \quad (4)$$

Here the number m describes the mechanism of wave coalescence. In the DPR model, $m = 1$ when the emission generates from the coalescence of two excited plasma waves and the polarization will be very weak; $m = 2$ when the emission generates from coalescence of an excited plasma wave and a low-frequency electrostatic wave and the polarization will be strong. Thus, the time profiles of f_s and Δf_s of the ZP stripes are associated with the variations of the plasma density and magnetic field. Both these quantities are perturbed by MHD waves, especially by standing and propagating sausage modes of coronal plasma structures.

Interpreting the observed ZP in terms of the DPR model, we can estimate the background plasma density and magnetic field. In this work, the ZP structure is moderate right polarization, the emission possibly generates from the coalescence of two excited plasma waves ($m = 2$), and the plasma density of the corresponding emission frequency (~3.0 GHz) is 2.8×10^{10} cm^{-3}. Taking that in the DPR resonant layer, the electron cyclotron frequency is s times lower than the emission frequency, one can estimate the value of the magnetic field in the layer. It requires the knowledge of the harmonic number s.

The harmonic number of a ZP stripe can be calculated if the ZP possesses at least three stripes (Yu et al. 2012). For an sth stripe and an $(s + i)$th stripe, the harmonic number is

$$s = \frac{i\,\delta_{s+i}}{\delta_s - \delta_{s+i}}, \quad (5)$$

where $\delta_s = \Delta f_s/f_s$, $\delta_{s+i} = \Delta f_{s+i}/f_{s+i}$, and $f_s = f_N$ is the observed frequency of the stripe. For the analyzed event, this was done by Yu et al. (2012). They calculated that the harmonic number of stripe 1 is $s \approx 10$ for both ZP1 and ZP2. This gives us a magnetic field of 50 G.

We estimate the Alfvén speed as $C_A \approx 700$ km s^{-1}. This value is consistent with typical estimations of Alfvén speed in solar coronal active regions obtained by the method of MHD coronal seismology (e.g., De Moortel & Nakariakov 2012). The absence of spatial resolutions in the observations of the discussed ZP does not allow us to determine the spatial location of the sources of individual ZP stripes. However, according to the estimations made in Chen et al. (2011) for a similar event when simultaneous imaging and spectroscopic observations over a large bandwidth were available, the sources of neighboring ZP stripes are separated by about 3 Mm. We may assume that in the discussed event, the spatial reparation of individual sources is of the same order. The oscillating wiggles of the ZP stripes can be caused by magnetoacoustic waves that perturb the magnetic field and plasma density. Magnetoacoustic waves with short periods are known to be present in the corona, from high spatial and time resolution observations during eclipses (Williams et al. 2001; Cooper et al. 2003). The waves are present in the corona in both standing and propagating forms. If the observed ZP wiggling is produced by a propagating wave, the detected oscillation period, about 1 s, and the estimated value of the Alfvén speed, about 700 km s^{-1}, allow us to estimate the wavelength. In particular, phase speeds of fast magnetoacoustic waves guided by coronal plasma non-uniformities are of the order of the Alfvén speed in the non-uniformity (e.g., Roberts et al. 1984). For example, such a quasi-periodic fast wave train could result from an impulsive excitation (e.g., Nakariakov et al. 2004) with the characteristic period given by the ratio of the transverse spatial scale of the waveguiding plasma structure and the Alfvén speed. Thus, the wavelength of propagating fast waves with a period of about 1 s is about 1 Mm. In the case of the slow magnetoacoustic wave, taking into account that in the corona the sound speed is lower than the Alfvén speed, the wavelength becomes even shorter than 1 Mm. Thus, if the oscillation is caused by a propagating magnetoacoustic wave, neighboring ZP stripes, separated by several Mm, would be positioned at different phases of the perturbation. Therefore, neighboring ZP stripes would wiggle with a significant phase difference that is not detected. Consequently, we rule out the interpretation of the ZP wiggling in terms of propagating waves. On the other hand, in a global standing mode, all segments of the waveguiding plasma non-uniformity oscillate in phase. Moreover, in a global sausage mode of sufficiently thin field-aligned plasma non-uniformities, the period is determined by the transverse size of the plasma non-uniformity and is almost independent of its longitudinal size (Kopylova et al. 2007; Nakariakov et al. 2012). Taking that the period of the detected oscillations is 1 s, we obtain that the required spatial size of the wave-guiding plasma non-uniformity with the estimated value of the Alfvén speed is about 1 Mm. This value is a typical minor radius of an active region loop. Consequently, the observed ZP wiggling can be associated with fast magnetoacoustic oscillations in the flaring active region. Moreover, the established lack of a significant phase shift between oscillations of different stripes that are coming from different spatial locations indicates that the MHD oscillation is likely to be standing. The above suggests that the detected ZP wiggles are caused by a standing sausage oscillation. This conclusion is supported by the finding that both the instant frequencies of individual stripes and their spectral separations oscillate with the same periods. This is consistent with a sausage oscillation that perturbs both the plasma density and magnetic field (Nakariakov et al. 2012). More information could be obtained from the analysis of the phase relationship between the instant frequencies of individual stripes and their spectral separations, but such a study requires an observational example of a ZP with higher-amplitude wiggling.

The work is supported by NSFC grant No. 11221063, 11273030; MOST grant No. 2011CB811401; and the National Major Scientific Equipment R&D Project ZDYZ2009-3. This research was also supported by the Marie Curie PIRSES-GA-2011-295272 *RadioSun* project, the European Research Council under the *SeismoSun* Research Project No. 321141 (V.M.N.), grant 8524 of the Ministry of Education and Science of the

Russian Federation (V.M.N.), and the Kyung Hee University International Scholarship (V.M.N.).

REFERENCES

Aschwanden, M. J. 1987, SoPh, 111, 113
Chen, B., Bastian, T. S., Gary, D. E., & Jing, J. 2011, ApJ, 736, 64
Chen, B., & Yan, Y. 2007, SoPh, 246, 431
Chernov, G. P. 2006, SSRv, 127, 195
Chernov, G. P., Markeev, A. K., Poquerusse, M., et al. 1998, A&A, 334, 314
Chernov, G. P., Yan, Y. H., Fu, Q. J., & Tan, C. M. 2005, A&A, 437, 1047
Chernov, G. P., Yasnov, L. V., Yan, Y.-H., & Fu, Q.-J. 2001, ChJAA, 1, 525
Cooper, F. C., Nakariakov, V. M., & Williams, D. R. 2003, A&A, 409, 325
Delaboudinière, J.-P., Artzner, G. E., Brunaud, J., et al. 1995, SoPh, 162, 291
De Moortel, I., & Nakariakov, V. M. 2012, RSPTA, 370, 3193
Fu, Q., Qin, Z., Ji, H., & Pei, L. 1995, SoPh, 160, 97
Fu, Q. J., Ji, H. Q., Qin, Z. H., et al. 2004, SoPh, 222, 167
Handy, B. N., Acton, L. W., Kankelborg, C. C., et al. 1999, SoPh, 187, 229
Isobe, H., Kubo, M., Minoshima, T., et al. 2007, PASJ, 59, 807
Jelínek, P., Karlický, M., & Murawski, K. 2012, A&A, 546, A49
Karlický, M. 2013, A&A, 552, A90
Karlický, M., Mészárosová, H., & Jelínek, P. 2013, A&A, 550, A1
Kim, S., Nakariakov, V. M., & Shibasaki, K. 2012, ApJ, 756, L36
Kopylova, Y. G., Melnikov, A. V., Stepanov, A. V., Tsap, Y. T., & Goldvarg, T. B. 2007, AstL, 33, 706
Kupriyanova, E. G., Melnikov, V. F., Nakariakov, V. M., & Shibasaki, K. 2010, SoPh, 267, 329
Kuznetsov, A. A. 2008, SoPh, 253, 103
Kuznetsov, A. A., & Tsap, Y. T. 2007, SoPh, 241, 127
LaBelle, J., Treumann, R. A., Yoon, P. H., & Karlicky, M. 2003, ApJ, 593, 1195
Linnell Nemec, A. F., & Nemec, J. M. 1985, AJ, 90, 2317
Mariska, J. T. 2006, ApJ, 639, 484
Nakajima, H., Nishio, M., Enome, S., et al. 1994, IEEEP, 82, 705
Nakariakov, V. M., Arber, T. D., Ault, C. E., et al. 2004, MNRAS, 349, 705
Nakariakov, V. M., Hornsey, C., & Melnikov, V. F. 2012, ApJ, 761, 134
Nakariakov, V. M., Inglis, A. R., Zimovets, I. V., et al. 2010, PPCF, 52, 124009
Nakariakov, V. M., & Melnikov, V. F. 2009, SSRv, 149, 119
Nakariakov, V. M., Pascoe, D. J., & Arber, T. D. 2005, SSRv, 121, 115
Ning, Z., Fu, Q., & Lu, Q. 2000a, A&A, 364, 853
Ning, Z., Fu, Q., & Lu, Q. 2000b, PASJ, 52, 919
Roberts, B., Edwin, P. M., & Benz, A. O. 1984, ApJ, 279, 857
Scargle, J. D. 1982, ApJ, 263, 835
Tajima, T., Sakai, J., Nakajima, H., et al. 1987, ApJ, 321, 1031
Tan, B., Yan, Y., Tan, C., & Liu, Y. 2007, ApJ, 671, 964
Tan, B., Zhang, Y., Tan, C., & Liu, Y. 2010, ApJ, 723, 25
Williams, D. R., Phillips, K. J. H., Rudawy, P., et al. 2001, MNRAS, 326, 428
Yan, Y. H., Fu, Q. J., Liu, Y. Y., & Chen, Z. J. 2002, in The 10th European Solar Physics Meeting, Solar Variability: From Core to Outer Frontiers, Vol. 1, ed. A. Wilson (ESA SP-506; Noordwijk: ESA Publication Division), 375
Yan, Y. H., Huang, J., Chen, B., & Sakurai, T. 2007, PASJ, 59, 815
Yu, S., Yan, Y., & Tan, B. 2012, ApJ, 761, 136
Yuan, D., Nakariakov, V. M., Chorley, N., & Foullon, C. 2011, A&A, 533, A116
Zaitsev, V. V., & Stepanov, A. V. 2008, PhyU, 51, 1123
Zheleznyakov, V. V., & Zlotnik, E. Y. 1975, SoPh, 44, 461
Zlotnik, E. Y., Zaitsev, V. V., Aurass, H., Mann, G., & Hofmann, A. 2003, A&A, 410, 1011